Available online at www.eccomasproceedia.org
Eccomas Proceedia COMPDYN (2023) 186-195

ECCOMAS
Proceedia

COMPDYN 2023
9th ECCOMAS Thematic Conference on
Computational Methods in Structural Dynamics and Earthquake Engineering
M. Papadrakakis, M. Fragiadakis (eds.)
Athens, Greece, 12-14 June 2023

DESIGN AND PERFORMANCE OF A PASSIVE VIBRATION CONTROL DEVICE FOR HAWT

E. Sorge[1], C. Riascos[2], N. Caterino[1,2], C. Demartino[3], C.T. Georgakis[4]

[1] Department of Engineering, University of Naples Parthenope, Napoli, Italy
ettore.sorge@studenti.uniparthenope.it

[2] Institute of Technologies for Construction, Italian National Research Council (CNR), San G. Milanese, Milan, Italy

[3] University of Roma Tre, Roma, Italy

[4] Department of Engineering, Aarhus University, Aarhus, Denmark

Abstract

This study proposes an innovative technique for reducing wind-induced stress at the base of a horizontal axis wind turbine (HAWT) and its foundation. The technique involves the use of a relaxed base constraint composed of rotational springs and friction devices in parallel, which dissipate energy to reduce bending moment demand while limiting displacement increase within acceptable limits. The aim of this study is the evaluation of a HAWT controlled by a rotational friction damper (RFD) under different wind load conditions for which the turbine is also operational, and studying the effectiveness of the proposed technique in multiple states. In this direction, spectrum compatible wind loads have been generated through the use of the QBlade® software and the European standard IEC61400-1. An optimization procedure has been performed to identify the characteristics of the device providing a satisfactory dynamic response of the turbine against all the evaluated load cases.
The results of nonlinear numerical analyses with a 5 MW NREL wind turbine demonstrate that the proposed system significantly reduces the bending moment at the base compared to the conventional 'fixed base' configuration. The proposed system confirms the promising potential of achieving a considerable reduction of the bending moment at the base compared to conventional 'fixed base' configuration.

Keywords: Rotational friction damper (RFD), vibration control, nonlinear optimization, wind turbine onshore

ISSN:2623-3347 © 2023 The Authors. Published by Eccomas Proceedia.
Peer-review under responsibility of the organizing committee of COMPDYN 2023.
doi: 10.7712/120123.10397.20597

1 INTRODUCTION

Onshore wind turbines are electromechanical systems that harness the kinetic energy of wind to produce electrical power. These devices comprise various components, such as the rotor assembly, aerodynamic blades, central hub, powertrain, electrical generator, and control system. The conversion of mechanical energy into electrical energy occurs through the powertrain and generator. The global wind energy sector is experiencing accelerated growth, driven in part by an intensified emphasis on sustainability and the mitigation of greenhouse gas emissions. According to the [1], installed wind power capacity worldwide reached 837 GW by the end of 2021. Europe remains the leader in the wind market, with a 48% market share, followed by China with 44%, while the US has 9% market share. However, there are also other emerging countries that are seeing significant growth in the wind market, such as India, Brazil and Mexico. Onshore wind turbines account for most of the world's installed wind power capacity. In particular, horizontal axis wind turbines (HAWT) are the most common, accounting for over 97% of installed capacity. The efficiency of onshore wind turbines depends on several factors, such as wind speed, air density, blade length, and the angle of incidence of the blades with respect to the wind.

To enhance energy generation efficiency, the wind energy industry is transitioning towards the fabrication of larger wind turbine towers. This shift, however, presents challenges related to increased structural vibrations and the subsequent amplification of stress transfer to the foundational support system. In this regard, the application of structural control devices has shown their capability to effectively mitigate structural vibrations in high wind towers may prove to be a valuable tool. Some studies have been focused on the energy dissipation to damp vibrations at the nacelle of the HAWT ([2], [3],[4]) other researchers have addressed tower vibration control at the interface tower-foundation. Among those works highlights that developed by Di Paolo *et al.* [5], introduced a passive control methodology that employs a rotational friction damper (RFD) to enhance the structural stability of towers. The RFD is strategically positioned at the base of the tower, working in conjunction with a rotational spring to optimize energy dissipation and to give re-centering capability to the whole restraint. Dissipating energy, the RFD mitigates the moment response at the base, while the spring primarily functions to reorient the tower to its original position, ensuring structural resilience. Fig.1 shows a schematic representation of the tower equipped with the control system (RB), where the stiffness of the rotational spring (k_s) and the strength of the RFD ($M_{fr,y}$) are the design parameters of the devices.

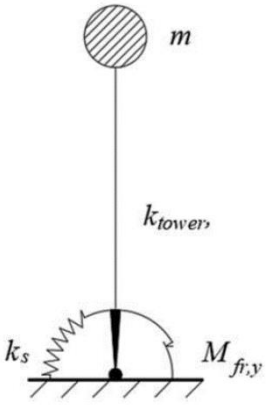

Figure 1: Schematic representation of the wind tubine tower equipped with the RFD and rotational springs (m is the mass of the nacelle and k_{tower} is the stiffness of the tower)

In this investigation, the objective is to expand upon previous research by focusing on three crucial aspects: refining the numerical model, introducing a potential design criterion, and

improving the generation of wind history simulations. The performance of the control system was tested under the action of wind corresponding to an operative scenario for the turbine. Spectrum compatible wind loads at the top of the turbine have been generated through the use of the QBlade® software and the European standard IEC61400-1. The so-obtained force histories were then applied to the structural model deployed in Matlab ([6]) and Simulik to obtain the non-linear system response (RFD). Finally, the design the control system at the base was obtained by performing an optimisation aiming at finding the maximum reduction of moment demand at the base of the HAWT in a pre-defined searching space.

2 BASELINE OF THE CASE-STUDY

A comprehensive analysis was conducted using a dynamic model derived from a 5 MW wind turbine prototype developed by the National Renewable Energy Laboratory (NREL). This prototype is considered a standard reference in the wind energy research field due to its widespread acceptance and adoption by the scientific community. The tower specifications are reported in [7] and are listed in Tab.1. The NREL-5MW is a three-bladed, variable-speed system with a rotor diameter of 126 m and a height at the hub (z_{hub}) of 90 m (Fig.2a). The cut-in, rated, and cut-out wind speeds represent distinct operational thresholds for a wind turbine, each of which is associated with corresponding blade pitch angle adjustments. Specifically, the cut-in wind speed is 3 m/s, at which point the turbine commences power generation with an optimal blade pitch angle for low wind speeds. The rated wind speed, at 11.4 m/s, signifies the velocity at which the turbine produces its maximum rated output, facilitated by a blade pitch angle configured for peak efficiency. Lastly, the cut-out wind speed is 25 m/s, beyond which the turbine ceases operation by adjusting the blade pitch angle to a protective position that prevents potential damage due to excessive wind force.

Each turbine blade consists of eight elements (Fig.2b), where each element has a different airfoil design (Fig.1b), and the maximum chord is 4.652 m. Blade pitch varies from 0° to 90° depending on wind speed and turbine scenario. When the turbine is stationary (parked scenario), i.e., the rotor is not rotating, the blades have a pitch angle of 90°. When the turbine is running (operative scenario) the pitch angle varies between 0° and 23.45°.

The tower, with a total height of 87.60 m, consists of a hollow tubular section with an outside diameter that varies with height. The external diameter and the thickness are variable along the height, respectively from 6.00 to 3.87 m and from 27 to 19 mm, starting from the base. The mass of the tower accounts for structural and non-structural components.

Table 1: Properties of NREL 5-MW Baseline Wind Turbine

Number of blades	3	Rotor, Hub Diameter	126,3 m
Cut-in/rated/cut-out wind speed	3/11.4/25 m/s	Hub Height	90 m
Cut-in/rated rotor speed	6.9/12.1 rpm	Tower top diameter	3.87 m
Rotor Mass	110 Mg	Tower base diameter	6.00 m
Nacelle Mass	240 Mg	Thickness bottom	27 mm
Tower Mass	347 Mg	Thickness top	19 mm

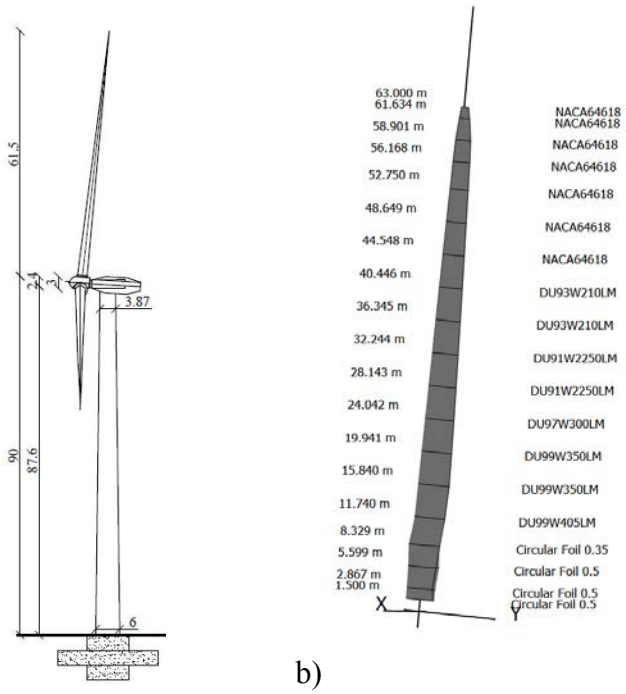

a) b)

Figure 2: NREL 5 MW wind turbine. a) Lateral view of Tower (dimensions in m); b) rotor-blade, with type of aerofoil used

The wind tower with fixed base (FB) has a fundamental frequency of 0.28 Hz. The control system installed at the base of the tower (Fig. 1) changes the modal behaviour of the tower. Depending on the device configuration, the HAWT-RFD can present a fundamental frequency until around the 30% of the fundamental frequency of the HAWT with fixed base.

3 GENERATION OF WIND ACTIONS

The cut-out wind speed is deemed to be of paramount importance concerning the maximal stress exerted on the tower structure. Consequently, for the purpose of evaluating the control efficiency, a nominal velocity of 25 m/s is selected in the present study.

Wind can be characterized as a stochastic process within a random field, signifying that it exhibits spatial and temporal random variations in both speed and direction. More precisely, wind can be mathematically represented as the sum of a mean intensity and a fluctuating component, with the latter accounting for the inherent uncertainty and variability in wind behavior across the field. To analyse the correlation between these spatial and temporal variations, the concept of coherence function can be employed. Wind time histories applied to the blades were generated using Qblade software [8] in accordance with [9].

After preliminary studies, the wind parameters were chosen based on the most critical conditions, in terms of vibration, for the HAWT. The wind turbine class considered is I for a turbulence category A, according to [9]. The average velocity component was considered to be 25 m/s, which corresponds to a velocity at the hub V_{hub}. For the turbulent components, the extreme turbulence model (ETM) is adopted following [9]. The ETM uses the normal wind profile (NWP) that is a power law wind profile is adopted:

$$V(z)=V_{hub}(z/z_{hub})^{0.2} \tag{1}$$

and the turbulence longitudinal component standard deviation are:

$$\sigma_1 = I_{ref}(0.75\ V_{hub} + 5.6) \quad (2)$$

where I_{ref} depends on the turbine class, and it is equal to 0.18 for the assumed conditions [9]. The turbulence model was chosen according to the Kaimal spectrum [10].

Five distinct wind fields, each 10 minutes long, were generated using random seeds to create unique stochastic realizations, capturing the random variability of aeroelastic forces under different conditions. As an example, the wind time history at the hub and a sample of the instantaneous turbulent wind field for the first generated wind field are shown in Fig 3a and Fig 3b.

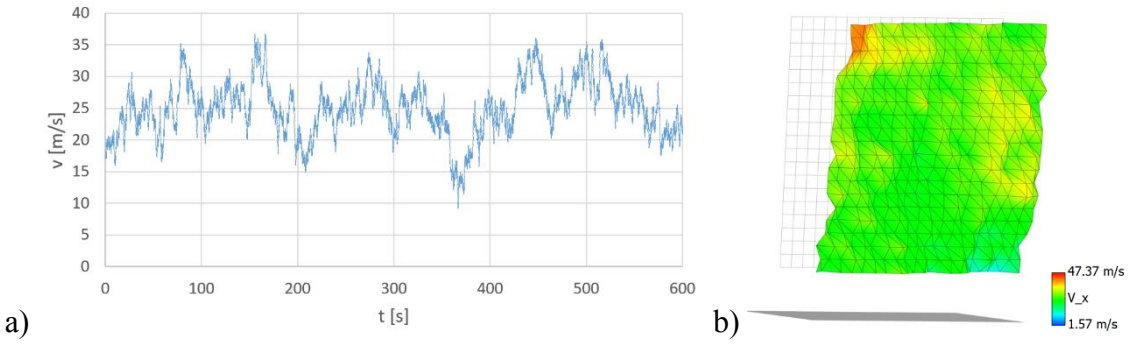

a) b)

Figure 3 a) Time-history of the wind speed with average of 25 m/s; b) example of the instantaneous turbulent wind field for the described velocity condition centred on the hub axis.

Upon acquiring the wind speed fields, they were incorporated into QBlade for analysis, facilitating the determination of force history to be applied at the tower head, as shown in Fig.4a. The aerodynamic response of the HAWT rotor blades was evaluated in the time domain. For each of the five distinct cases, the time histories of thrust (horizontal force in the main wind direction) exerted on the rotor and moments experienced at the hub were computed using QBlade. An example of the rotor thrust time history for the first generated wind field is shown in Fig.4b.

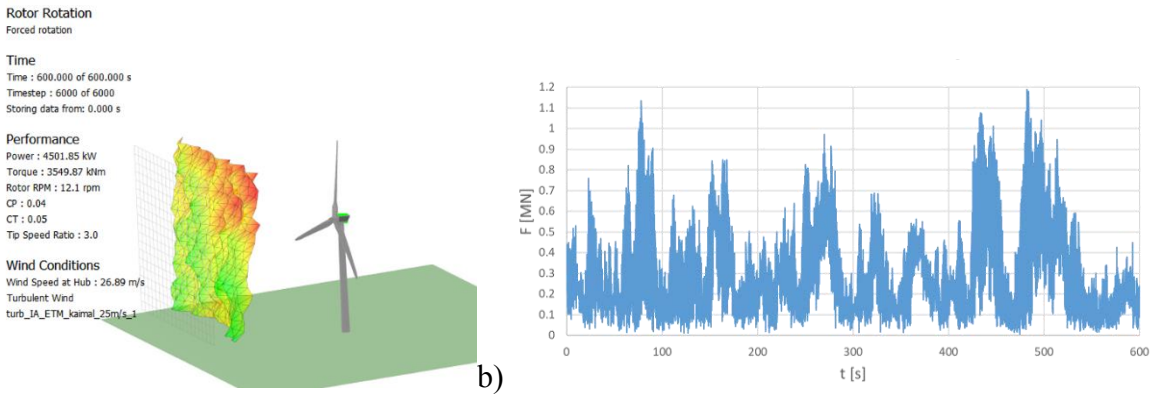

a) b)

Figure 4 a) Simulation in Qblade; b) thrust at the hub to pitch angle 23.47°

4 STUCTURAL MODEL

Each thrust and moment time histories are then applied to the top of the tower in the structural model to evaluate the bending moment time histories at the base of the tower. In light of the tower variable cross-sectional geometry and considerable height, the HAWT tower was discretized into several consecutive elastic elements, resulting in a multi-degree-of-freedom system. Both translation and rotation DOFs, denoted as $\theta_i(t)$ and $u_i(t)$ for *i*-th height, are considered while the axial behavior is neglected. Additionally, the rotation at the base of the wind turbine generator (WTG) was denoted as $\theta_0(t)$. The tower modal damping ratio (ζ) is taken as 1% ([7]). The mass of the WTG was determined using a diagonal matrix, which incorporates the generator mass at the corresponding degrees of freedom, as described in detail in [5]. By including the effect of the control device, the equation of motion describing the WTG-RFD system is:

$$\boldsymbol{M\ddot{u}} + \boldsymbol{C\dot{u}} + \left(\boldsymbol{K} - \boldsymbol{P_p}\right)\boldsymbol{u} + g_{fr}\left(t, \dot{\theta}_0\right)\boldsymbol{\Gamma_{fr}} = \boldsymbol{F_a}(\boldsymbol{t}) \tag{3}$$

where, $\boldsymbol{M}$, $\boldsymbol{C}$ and $\boldsymbol{K}$ are the WTG mass, damping and stiffness matrices, respectively. $\boldsymbol{P_p}$ approximates the second order effects of tower deflection, $\boldsymbol{F_a}(t)$ is the aeroslatic force and $g_{fr}\left(t, \dot{\theta}_0\right)$ is the rotational resistance at the base due to the RFD, accompanied by its associated influence vector $\boldsymbol{\Gamma_{fr}}$. A widely used representation for the determination of $g_{fr}\left(t, \dot{\theta}_0\right)$ is that obtained by using Coulomb friction, whereby $g_{fr}\left(t, \dot{\theta}_0\right) = M_{fr}\left|\dot{\theta}_0\right| sign\left(\dot{\theta}_0\right)$ [11]. Since this term turns the system of ordinary differential equations into a nonlinear system, this equation was solved numerically using Simulink with a Dormand Prince integration algorithm with a variable time step (dt). Nonetheless, the friction term's abrupt directional changes necessitated a substantial reduction in the time step (dt), which significantly increased the computational calculation time to maintain an acceptable level of accuracy in the integration process. To mitigate this numerical effect, the terms $|\dot{\theta}_0|$ and $sign(\dot{\theta}_0)$ were replaced by equivalent smoothed terms. The term $|\dot{\theta}_0|$ is represented through the smoothed function $\sqrt{|\dot{\theta}_0|^2 + \epsilon}$. The parameter ϵ used provides a fit of approximately 99% with respect to the reference term, while substantially enhancing the computational efficiency for small amplitude rotations. Furthermore, the term $sign(\dot{\theta}_0)$ was replaced by the function $tanh(\dot{\theta}_0\alpha)$, where tanh is the hyperbolic tangent function, α is a shape parameter that allows scale the sensitivity of the friction force to variations of $\dot{\theta}_0$. Given that the model of the WTG-RFD system should represent different dynamic characteristics, including both extremely low and considerable high values for the rotational stiffness and the frictional moment of the RFD, a normalization of $\dot{\theta}_0$ is obtained through α. For this purpose, an equivalent rms value of the rotation $\theta_0(t)$ of the tower is estimated using:

$$\theta_{rms} = \frac{F_m H}{k_s} \tag{4}$$

where F_m represents the rms of the aeroelastic force at hub level (z_{hub}). Ω_{eq} is obtained by multiplying θ_{rms} by the fundamental frequency of the WTG-RFD system:

$$\omega_n = \sqrt{\frac{k_s}{I_\theta}} \tag{5}$$

$$\Omega_{eq} = \omega_n \theta_{rms} \tag{6}$$

where I_θ is the rotational inertia of the complete system. The parameter α is invertedly proportional to Ω_{eq}. However, the friction contribution must be activated from a fraction (γ<<1) of Ω_{eq}

since the approximation of the plastic effect must occur since low vibration amplitudes as shown in:

$$G_{fr}\left(t,\dot{\theta}_0\right) = \sqrt{\left|\dot{\theta}_0\right|^2 + \varepsilon}\,\tanh\left(\frac{\dot{\theta}_0}{\gamma\Omega_{eq}}\right) \tag{7}$$

Considering a wide group of different types of RFD (k_s, $M_{fr,y}$), and conserving admissible stability and accuracy criteria, a value of γ of 2% is set. Consequently, each numerical integration was executed efficiently, with an average computational duration of 5 seconds per case, considering a 10-minute wind load scenario. A Intel Core i7-6700 reference computer with a nominal processing frequency of 3.4 GHz was used.

Additionally, the input signals incorporated an initial transition phase achieved through a sigmoidal function and a final free-vibration phase. It is worth mentioning that this last phase allows to evaluate residual displacements.

5 RFD DESIGN AND OPTIMIZATION

To determine the adequate combination of k_s and $M_{fr,y}$ for an RFD-WTG under different wind load scenarios is a challenging task since these parameters determine the performance of the control device. To solve this issue, an optimization that minimizes the base moment for each load field was considered in this study. The objective function was defined as the mean ratios between the maximum moment of the RFD-WTG system and that of the WTG with fixed base configuration:

$$f_{obj}(x) = \frac{1}{N}\sum_{i=1}^{N}\frac{max\left(\left|M_{RB}^{(i)}(t,x)\right|\right)}{max\left(\left|M_{FB}^{(i)}(t)\right|\right)} \tag{10}$$

where $x = \left[k_s, M_{fr,y}\right]^T$ is a vector that includes the parameters of the device. The upper and lower values of x are:

$$[k_{tower}/2\,,\, M_{FB}/20]^T \le x \le [3\,k_{tower}, M_{FB}/2]^T \tag{9}$$

It is worthy to mention that the optimization (i.e. find the minimum of the objective function, Eq. 10) was performed with the [6] optimization toolbox *fmincon* adopting an *interior-point* algorithm [6].

Although the general purpose of the study is to determine the characteristics of the HAWT-RFD system for a several wind cases (global approach), the analysis also encompasses the identification of individual RFD characteristics for each specific wind case, employing a localized methodology. Therefore, the objective function is limited to the $max\left(\left|M_{RB}^{(i)}(t,x)\right|\right)/max\left(\left|M_{FB}^{(i)}(t)\right|\right)$ function and the same limits were used for the vector of x variables described in Eq. (8).

6 RESULTS

The analyses were carried out for the following range of input parameters: rotational friction device resistance $M_{fr,y}$ in the range of 0.05 to 0.50 times the value of $M_{FB,avg}$ (i.e., the average of the five peak moments at the base of the tower in the FB configuration) and the rotational

stiffness due to the vertical springs k_s from 0.4 to 2.6 times the value of k_{tower} (i.e. the rotational stiffness of the tower).

The optimisation process determined the best pair of RFD characteristics for both local approach and global approaches. In each case, the optimisation process was initiated at the centre of the grid and then the interior-point algorithm, through gradient determination, achieved the correct identification of the momentum-minimising point at the base of the system with control. Complementarily, the momentum reduction field at the base was elaborated through a structured mesh over the x-domain, in order to illustrate the optimisation process and validate the performance of the same, as shown by the contour lines in Fig. 5. These lines indicate the position of the points of equal performance in terms of maximum moment ratio for each of the 5 cases. For each case, a significant reduction in the maximum moment demand is achieved, up to about 20%. In this figure, the contour lines are quite different for each case, highlighting how the performance of the proposed system is not load case independent. However, this is common in structural engineering, so one of the scopes of this research is that of giving a path to find an optimal compromise configuration.

Applying the optimisation algorithm, the best solution (i.e., the one that provides the best reduction in bending moment against the whole set of cases) was found. The solution, highlighted using the star symbol (global solution), corresponds to a pair of values ($M_{fr,y}$, k_s) equal to $M_{fr,y}$ =0.1 $M_{FB,avg}$ = 10 MNm and k_s=2.05 k_{tower} = 18630 MNm/rad. The red circle (local solution) on the figures indicates the pair of values ($M_{fr,y}$, k_s) that leads to the highest moment reduction for the individual case.

For Case 1 (Fig.5a) and Case 4 (Fig.5d), there is no great difference between the "local" and "global" solution. For the other three cases, the compromise configuration leads to a small – physiologic - worsening in the moment reduction. A summary of the local and global dimensionless solutions is shown in Fig5f.

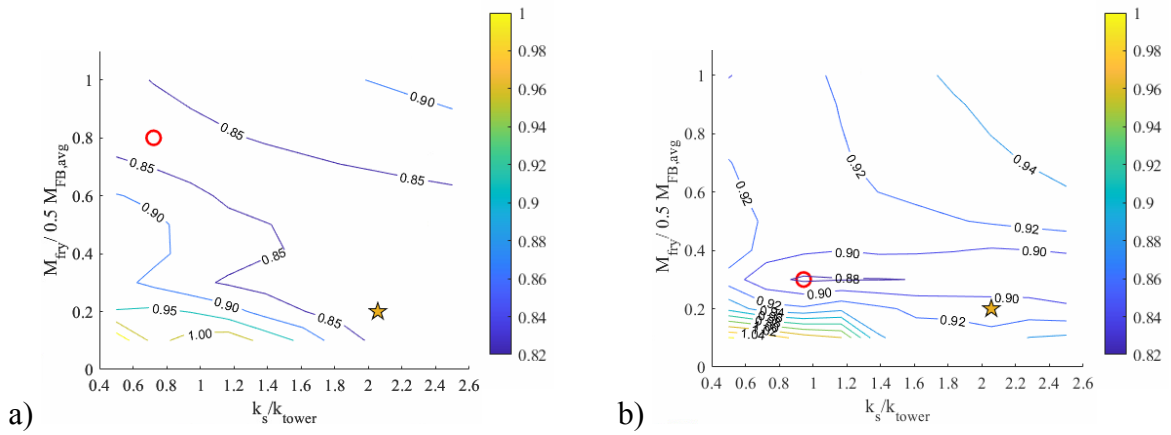

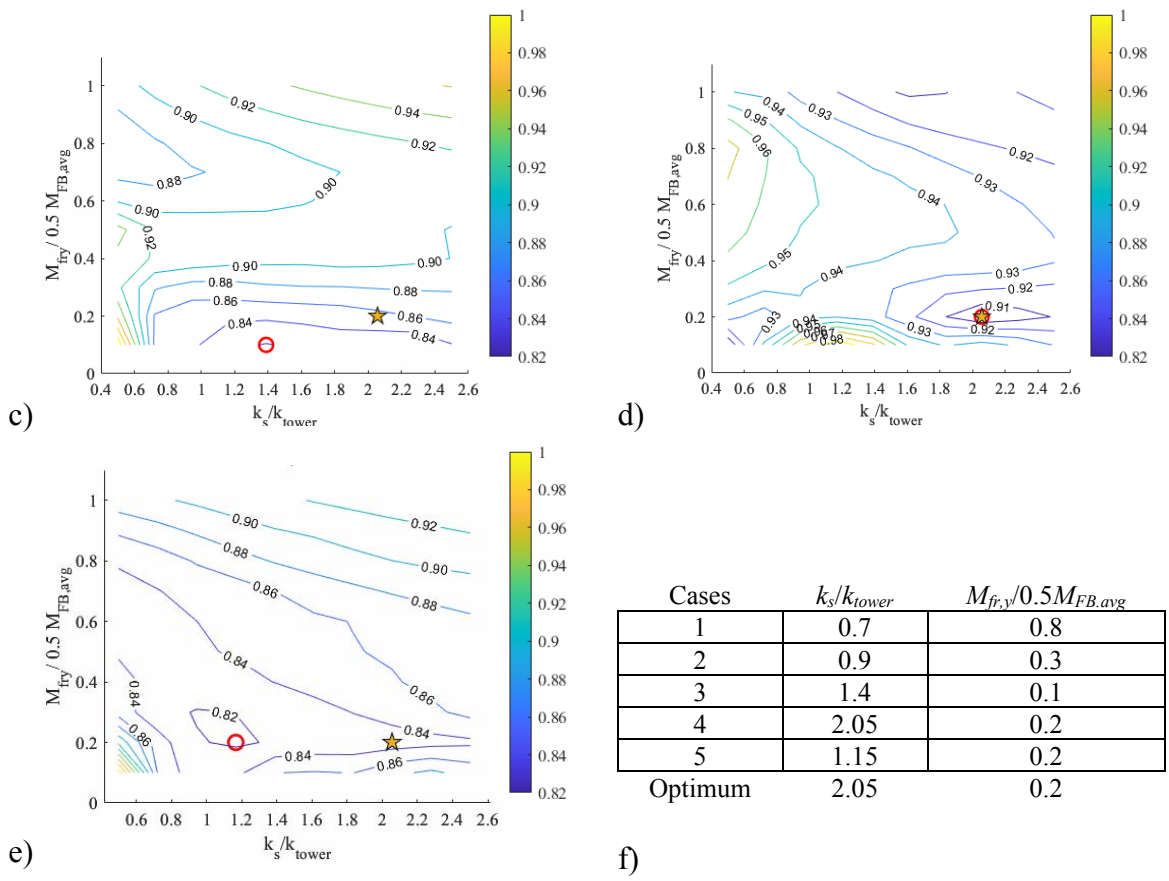

Cases	k_s/k_{tower}	$M_{fr,y}/0.5M_{FB.avg}$
1	0.7	0.8
2	0.9	0.3
3	1.4	0.1
4	2.05	0.2
5	1.15	0.2
Optimum	2.05	0.2

f)

Figure 5. Percentage of moment reduction in the control configurations examined for a) Case1, b) Case2, c) Case3, d) Case4, e) Case5. The red circle indicates the optimum value for the individual case, the star indicates the optimum compromise solution for all cases; f) Summary table of value pairs $M_{fr,\,y}$ and k_s, adimensionalized respectively with respect to $0.5M_{FB.avg}$ and k_{tower}.

7 CONCLUSIONS

In this study, numerical results are presented for the design and optimization of a passive control system implemented at the base of an onshore Horizontal Axis Wind Turbine (HAWT). This control system aims to mitigate stress exerted on the tower and, subsequently, the foundation. The control strategy utilizes a Rotational Friction Damper (RFD) installed at the tower's base, working in parallel with a rotational spring. To assess the aerodynamic effects on the HAWT's structural model, the aerodynamic behaviour of the rotor was decoupled from the dynamic response of the structure. The aerodynamic response of a rotor subjected to five different wind loads was obtained by creating different wind fields in Qblade [8]. Then, the time-histories of thrust and moment forces at the hub were applied to numerical models to evaluate the structural response of the tower with and without the control system.

The proposed optimization identified the best RFD characteristics in the reduction of the moment demand at the base of the HAWT for either local (single wind case) and global (multiple wins cases) approaches. It was identified that the RFD was able to reduce this indicator up to the 80% of the moment with respect to FB configuration. This technique can be advantageous both in the case of repowering existing plants and for the construction of new plants.

Future improvements include considering the three-dimensional behaviour of the turbine in conjunction with its control system.

REFERENCES

[1] Global Wind Energy Council, https://gwec.net/wp-content/uploads/2022/04/Annual-Wind-Report-2022_screen_final_April.pdf, 2022.

[2] Z. Feng, Y. Huang, X. Hua, J. Dai, H. Jing, Vibration-Resistant Performance Study of a Novel Floating Wind Turbine with Double-Rope Mooring System and Stroke-Limited TMD. *Journal of Marine Science and Engineering*, 11(1), 58, 2023.

[3] Z. Jiang, Y. Xing, Load mitigation method for wind turbines during emergency shutdowns. *Renewable Energy*, 185, 978-995, 2022.

[4] Z. Zhao, K. Dai, E.R. Lalonde, J. Meng, B. Li, Z. Ding, G. Bitsuamlak, Studies on application of scissor-jack braced viscous damper system in wind turbines under seismic and wind loads. *Engineering Structures*, 196, 109294, 2019.

[5] M. Di Paolo, I. Nuzzo, N. Caterino, C. T. Georgakis, A friction-based passive control technique to mitigate wind induced structural demand to wind turbines. *Engineering Structures*, 232, 111744, 2021.

[6] MATLAB version 9.13.0.2049777, (R2022b) Update 2. Natick, The MathWorks Inc., Massachusetts, 2022

[7] J. Jonkman, S. Butterfield, W. Musial, G. Scott, Definition of a 5-MW Reference Wind Turbine for Offshore System Development. *Office of Energy Efficiency and Renewable Energy*, Washington, DC, USA, 2009.

[8] D. Marten, QBlade: a modern tool for the aeroelastic simulation of wind turbines. 2020.

[9] IEC 61400-1, *International Standards, Wind Turbines - Part 1: Design requirement*, 2009.

[10] J. C. Kaimal, J. C. J. Wyngaard, Y. Izumi, O. R Coté, Spectral characteristics of surface-layer turbulence. *Quarterly Journal of the Royal Meteorological Society*, 98(417), 563-589, 1972.

[11] L. Marino, A. Cicirello. Coulomb friction effect on the forced vibration of damped mass–spring systems. *Journal of Sound and Vibration* 535: 117085, 2022.